Article

Ligand Specificity of CS-35, a Monoclonal Antibody That Recognizes Mycobacterial Lipoarabinomannan: A Model System for Oligofuranoside–Protein Recognition

Christoph Rademacher, Glen K. Shoemaker, Hyo-Sun Kim, Ruixiang Blake Zheng, Hashem Taha, Chunjuan Liu, Ruel C. Nacario, David C. Schriemer, John S. Klassen, Thomas Peters, and Todd L. Lowary

J. Am. Chem. Soc., **2007**, 129 (34), 10489-10502• DOI: 10.1021/ja0723380 • Publication Date (Web): 02 August 2007

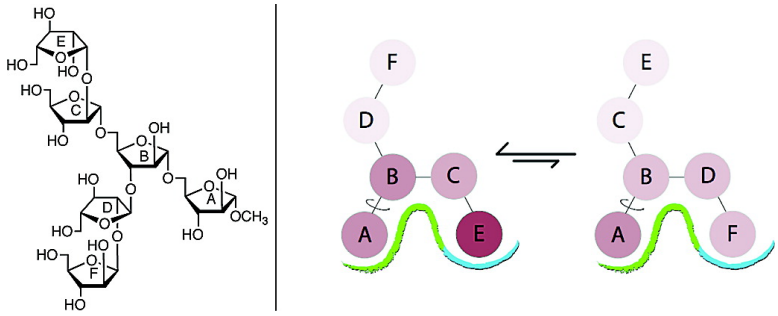

More About This Article

Additional resources and features associated with this article are available within the HTML version:

- Supporting Information
- Links to the 3 articles that cite this article, as of the time of this article download
- Access to high resolution figures
- Links to articles and content related to this article
- Copyright permission to reproduce figures and/or text from this article

View the Full Text HTML

J|A|C|S
ARTICLES
Published on Web 08/02/2007

Ligand Specificity of CS-35, a Monoclonal Antibody That Recognizes Mycobacterial Lipoarabinomannan: A Model System for Oligofuranoside−Protein Recognition

Christoph Rademacher,[†] Glen K. Shoemaker,[‡] Hyo-Sun Kim,[‡] Ruixiang Blake Zheng,[‡] Hashem Taha,[‡] Chunjuan Liu,[‡] Ruel C. Nacario,[‡] David C. Schriemer,[§] John S. Klassen,[‡] Thomas Peters,[†] and Todd L. Lowary*[,‡]

Contribution from the Alberta Ingenuity Centre for Carbohydrate Science and Department of Chemistry, The University of Alberta, Gunning-Lemieux Chemistry Centre, Edmonton, AB T6G 2G2, Canada, Institute of Chemistry, University of Lübeck, Ratzeburger Allee 160, 23538 Lübeck, Germany, and Department of Biochemistry and Molecular Biology, The University of Calgary, 3330 Hospital Drive NW, Calgary, Alberta T2N 4N1, Canada

Received April 3, 2007; E-mail: tlowary@ualberta.ca

Abstract: The CS-35 antibody is widely used in the characterization of glycans containing D-arabinofuranose residues, in particular polysaccharides present in the mycobacterial cell wall. A detailed understanding of the combining site of this antibody and the measurement of its binding to different ligands is of interest as this knowledge will have implications in the characterization of arabinofuranose-containing glycoconjugates that are increasingly recognized as important biological molecules. Of even greater significance is that an in-depth study of this carbohydrate−protein interaction will provide insights into the mechanisms by which oligosaccharides containing furanose rings are bound by proteins, an area that has, to date, received little attention. This system has been refractory to X-ray crystallography, and thus we report here a study of the interaction of CS-35 with its ligands using a combination of chemical synthesis, mass spectrometry, titration microcalorimetry, and NMR spectroscopy. Through these investigations we have established that the binding pocket recognizes, as a minimum epitope, a linear tetrasaccharide motif and that the residues at the reducing and non-reducing end of the oligosaccharide are essential for tight binding. The residue at the non-reducing end appears to be bound in an aliphatic pocket, whereas the rest of the tetrasaccharide interacts more strongly with aromatic amino acids.

Introduction

Infections by mycobacterial pathogens, including *Mycobacterium tuberculosis*, remain significant worldwide health threats. For example, it is estimated that one-third of the global population is infected with *M. tuberculosis* and each year tuberculosis and leprosy, which is caused by *M. leprae*, kill more than three million people combined.[1] The emergence of drug-resistant mycobacterial strains[2] and the increase in the number of immunocompromised individuals who are particularly susceptible to infection[3] have led to heightened interest in the identification of new drugs and vaccines for the treatment and prevention of these diseases.[4,5] The search for such therapeutic agents has, in turn, prompted increased research in the basic biochemistry of mycobacteria, and one area receiving significant attention is the cell wall of these organisms.[6]

The major component of the mycobacterial cell wall is the mycolyl−arabinogalactan complex, an arabinogalactan (AG) polysaccharide esterified with mycolic acids, branched lipids characteristic to mycobacteria, and other actinomycetes.[7] Another important cell wall component is an immunomodulatory polysaccharide, lipoarabinomannan (LAM).[8] These polysaccharides play critical roles in the survival and pathogenicity of the organism and possess a number of remarkable structural features.

[†] University of Lübeck.
[‡] The University of Alberta.
[§] The University of Calgary.

(1) (a) Paolo, W. F., Jr.; Nosanchuk, J. D. *Lancet Infect. Dis.* **2004**, *4*, 287−293. (b) Davies, P. D. O. *Ann. Med.* **2003**, *35*, 235−243. (c) Coker, R. J. *Trop. Med. Int. Health* **2004**, *9*, 25−40.
(2) (a) Nachega, J. B.; Chaisson, R. E. *Clin. Infect. Dis.* **2003**, *36*, S24−S30. (b) Wade, M. M.; Zhang, Y. *Front. Biosci.* **2004**, *9*, 975−994.
(3) De Jong, B. C.; Israelski, D. M.; Corbett, E. L.; Small, P. M. *Annu. Rev. Med.* **2004**, *55*, 283−301.
(4) (a) Zhang, Y. *Annu. Rev. Pharmacol. Toxicol.* **2005**, *45*, 529−564. (b) Biava, M.; Porretta, G. C.; Deidda, D.; Pompei, R. *Infect. Disord.: Drug Targets* **2006**, *6*, 159−172. (c) Jachak, S. M.; Jain, R. *Anti-Infect. Agents Med. Chem.* **2006**, *5*, 123−133.
(5) (a) Dietrich, J.; Lundberg, C. V.; Andersen, P. *Tuberculoisis* **2006**, *86*, 163−168. (b) Orme, I. M. *Vaccine* **2006**, *24*, 2−19. (c) Skeiky, Y. A. W.; Sadoff, J. C. *Nat. Rev. Microbiol.* **2006**, *4*, 469−476.
(6) Draper, P.; Daffe, M. The Cell Envelope of *Mycobacterium tuberculosis* with Special Reference to the Capsule and Outer Permeability Barrier. In *Tuberculosis and the Tubercle Bacillus;* Cole, S. T., Eisenach, K. D., McMurray, D. N., Jacobs, W. R., Jr., Eds.; American Society for Microbiology: Washington, DC, 2005; pp 261−273.
(7) Mahaptra, S.; Basu, J.; Brennan, P. J.; Crick, D. C. Structure Biosynthesis and Genetics of the Mycolic Acid-Arabinogalactan-Peptidoglycan Complex. In *Tuberculosis and the Tubercle Bacillus;* Cole, S. T., Eisenach, K. D., McMurray, D. N., Jacobs, W. R., Jr., Eds.; American Society for Microbiology: Washington, DC, 2005; pp 275−285.
(8) (a) Nigou, J.; Gilleron, M.; Puzo, G. *Biochemie* **2003**, *85*, 153−166. (b) Briken, V.; Porcelli, S. A.; Besra, G. S.; Kremer, L. *Mol. Microbiol.* **2004**, *53*, 391−403.

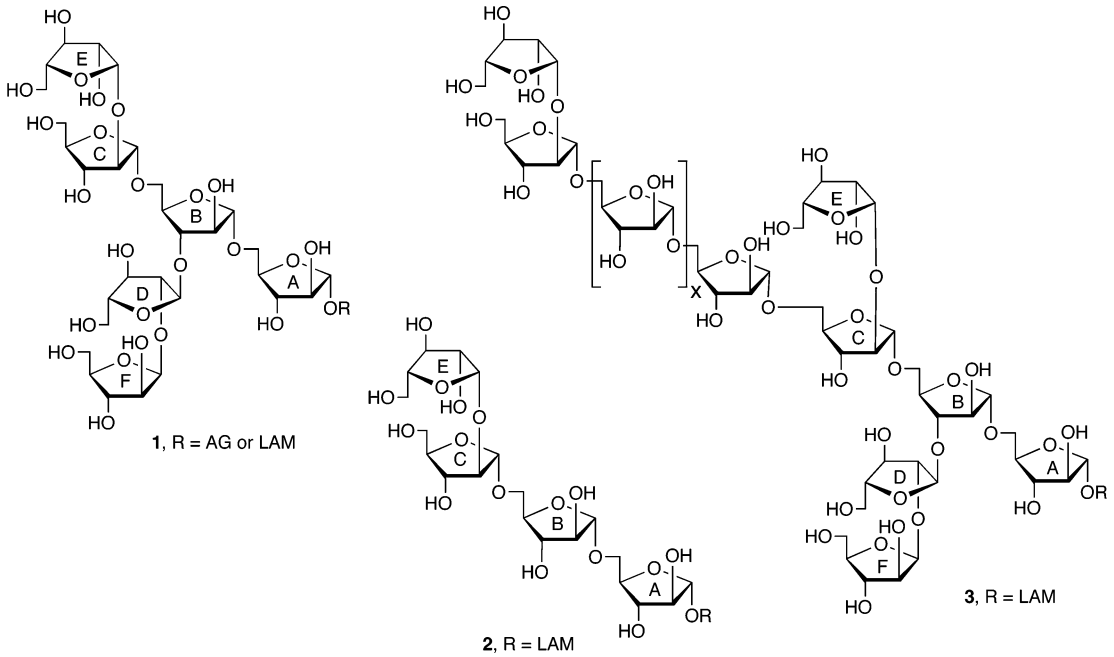

Figure 1. Structural motifs at the non-reducing termini of the arabinan domains in mycobacterial AG (**1**) and LAM (**2**, **3**). Rings are lettered to facilitate comparison.

In particular, both have an arabinan domain composed of α-(1→5), α-(1→3) and *β*-(1→2)-linked D-arabinofuranose (D-Ara*f*) residues.[6] This arabinan is located at the non-reducing end of both polysaccharides, and in the AG, its distal end is capped with the hexasaccharide motif Ara6 (**1**, Figure 1).[7] In LAM, either **1** or a related linear tetrasaccharide, Ara4 (**2**), is found at this terminus.[8] The presence of Ara4 in LAM has previously been attributed to incomplete branching during LAM biosynthesis. However, very recent structural work suggests that, at least in some mycobacterial species, this linear motif is attached to the non-reducing end of the Ara6 moieties.[9] For example, it has been proposed that an α-(1→5)-linked arabinan extends from residue C in **1**, which is then capped by a *β*-(1→2)-linked Ara*f* residue, thus generating a more highly branched structure, **3**.

Because humans do not produce arabinofuranose-containing glycoconjugates, the enzymes involved in mycobacterial arabinan biosynthesis have attracted attention as targets for drug action.[7,10] Work in this area has been bolstered significantly by the revelation that one of the drugs used to treat tuberculosis, ethambutol, acts by inhibiting at least one of the arabinosyltransferases (AraTs) involved in this process.[11] Over the past several years, a number of studies[12] have been undertaken not only to determine the genes encoding for these AraTs but also to establish unequivocally the protein targeted by ethambutol. These investigations have involved the analysis of polysaccharides isolated from mycobacteria treated with ethambutol or those from mutant organisms in which key genes have been deleted or truncated.[9,13] In many of these studies, a monoclonal antibody (mAb), CS-35, has played an important role in the characterization of the AG and LAM structures produced by these mutant or drug-treated organisms. This mAb, originally generated[14] against *M. leprae* LAM, also binds to LAM from other mycobacteria as well as AG.[15] Earlier investigations,[15] using competitive ELISA experiments with chemically synthesized arabinan fragments, revealed that this mAb binds motif **1** and **2**, thus suggesting that the protein interacts predominantly with residues A, B, C, and E. In support of this notion, a tetrasaccharide containing only residues A, B, D, and F was shown not to be a ligand.

Beyond these studies, nothing else is known about the fine ligand specificity of this mAb. Clearly, a more detailed picture of the CS-35 combining site and the quantitation of its binding to different ligands will have important implications in the characterization of mycobacterial arabinans. Of perhaps even greater significance, a more in-depth study of this carbohydrate−protein interaction will also provide insights into the manner in which proteins bind oligosaccharides containing furanose rings (oligofuranosides). A substantial body of structural work on oligosaccharide−protein interactions is available.[16] However, these investigations have nearly exclusively focused on complexes in which the glycan ligands contain only pyranose rings.

(9) Shi, L.; Berg, S.; Lee, A.; Spencer, J. S.; Zhang, J.; Vissa, V.; McNeil, M. R.; Khoo, K.-H.; Chatterjee, D. *J. Biol. Chem.* **2006**, *281*, 19512−19526.
(10) Lowary, T. L. *Mini-Rev. Med. Chem.* **2003**, *3*, 694−707.
(11) Belanger, A. E.; Besra, G. S.; Ford, M. E.; Mikusová, K.; Belisle, J. T.; Brennan, P. J.; Inamine, J. M. *Proc. Natl. Acad. Sci. U.S.A.* **1996**, *93*, 11919−11924.
(12) Berg, S.; Kaur, D.; Jackson, M.; Brennan, P. J. *Glycobiology* **2007**, *17*, 35R−56R.
(13) (a) Mikuová, K.; Slayden, R. A.; Besra, G. S.; Brennan, P. J. *Antimicrob. Agents Chemother.* **1995**, *39*, 2484−2489. (b) Khoo, K.-H.; Douglas, E.; Azadi, P.; Inamine, J. M.; Besra, G. S.; Brennan, P. J.; Chatterjee, D. *J. Biol. Chem.* **1996** *271*, 28682−28690. (c) Escuyer, V. E.; Lety, M.-A.; Torrelles, J. B.; Khoo, K.-H.; Tang, J.-B.; Rithner, C. D.; Frehel, C.; McNeil, M. R.; Brennan, P. J.; Chatterjee, D. *J. Biol. Chem.* **2001**, *276*, 48854−48862. (d) Zhang, N.; Torrelles, J. B.; McNeil, M. R.; Escuyer, V. E.; Khoo, K.-H.; Brennan, P. J.; Chatterjee, D. *Mol. Microbiol.* **2003**, *50*, 69−76. (e) Berg, S.; Starbuck, J.; Torrelles, J. B.; Vissa, V. D.; Crick, D. C.; Chatterjee, D.; Brennan, P. J. *J. Biol. Chem.* **2005**, *280*, 5651−5663. (f) Lee, R. E. B.; Li, W.; Chatterjee, D.; Lee, R. E. *Glycobiology* **2005**, *15*, 139−151. (g) Alderwick, L. J.; Radmacher, E.; Seidel, M.; Gande, R.; Hitchen, P. G.; Morris, H. R.; Dell, A.; Sahm, H.; Eggeling, L.; Besra, G. S. *J. Biol. Chem.* **2005**, *280*, 32362−32371. (h) Alderwick, L. J.; Seidel, M.; Sahm, H.; Besra, G. S.; Eggeling, L. *J. Biol. Chem.* **2006**, *281*, 15653−15661.
(14) Hunter, S. W.; Gaylord, H.; Brennan, P. J. *J. Biol. Chem.* **1986**, *261*, 12345−12351.
(15) Kaur, D.; Lowary, T. L.; Vissa, V. D.; Crick, D. C.; Brennan, P. J. *Microbiol. (Reading, U. K.)* **2002**, *148*, 3059−3067.

These oligopyranoside−protein complexes are typically stabilized by hydrogen bonding between the carbohydrate and protein, as well as van der Waals interactions between "hydrophobic" faces in monosaccharides and aromatic amino acids.[17] Far fewer reports have described details of complexes between proteins and oligofuranosides. To date, those systems receiving the most scrutiny have been enzymes involved in the processing of L-arabinofuranosides[18] and D-fructofuranosides.[19,20] Lectins[21] and transporter proteins[22] that bind to sucrose and related oligosaccharides containing D-fructofuranose moieties have also been studied. Although it is certain that complexes formed between oligofuranosides and proteins will share many similarities with their pyranoside counterparts (i.e., hydrogen bonds), differences could also be expected. For example, the monosaccharides most commonly found in naturally occurring oligofuranosides, arabinose and galactose, lack clear hydrophobic faces. Moreover, oligofuranosides are inherently more flexible[23] than oligopyranosides, and the importance of this increased mobility on the dynamics of binding is not understood.

Mindful of the above considerations, we view the mAb CS-35/arabinan interaction as an excellent model system for probing oligofuranoside−protein recognition. As part of a larger program directed at obtaining a molecular-level understanding of this interaction, we report here the use of oligosaccharide fragments of mycobacterial arabinan (**4**−**20**, Figure 2) to probe and quantitate the ligand specificity of this mAb. These investigations, which involved the use of state-of-the-art methods in chemical synthesis, mass spectrometry, and NMR spectroscopy, have provided key insights into this carbohydrate−protein complex. Efforts to characterize this complex by X-ray crystallography have been unsuccessful to date, due to difficulties in obtaining diffractable crystals.

Materials and Methods

Synthesis of Ligands. Oligosaccharides **4** and **6**−**20** were prepared as reported previously.[24] Pentasaccharide **5** was synthesized as outlined in Scheme 1 using an elegant method for the synthesis of β-arabinofuranosides recently reported by Boons and co-workers.[25] The known[24c] trisaccharide diol, **21**, was reacted with thioglycoside **22**[26,27] in the presence of *N*-iodosuccinimide and silver triflate to afford the expected pentasaccharide **23** in 92% yield. Deprotection was achieved in two steps, first by treatment with tetra-*n*-butylammonium fluoride in THF (to give **24**) followed by hydrogenolysis of the benzyl ethers over $Pd(OH)_2$/C in methanol. The target **5** was obtained in 51% overall yield from **23**.[26]

Production of mAb CS-35. The cell line that produces mAb CS-35 was obtained from Dr. John S. Spencer of Colorado State University under the terms of the NIH-sponsored contract Tuberculosis Research Materials and Vaccine Testing Contract (NO1, AI-75320). A stock vial of mAb CS-35 cells was removed from storage in liquid nitrogen and rapidly thawed in a water bath before the cells were transferred to a 15 mL conical tube, and BD media (10 mL, BD Bioscience) was added slowly. The number of viable cells was determined using 0.1% trypan blue stain in a 1:1 ratio and a hemocytometer. The cells were then resuspended in media to the desired concentration (500 000−1 000 000 cells/mL) after centrifugation. Next, the cells (10 mL) were transferred to a 25 mL flask (T-25) and placed in a humidified CO_2 (8%) incubator for 2 days at which point they were split in a 1:10 ratio (established culture:fresh media) until viability was greater than 95%. The cells (3×10^7) were resuspended in BD media (15 mL) containing 20% heat inactivated fetal bovine serum (HI-FBS) and transferred to the small compartment of an artificial mouse (a CELLine device, BD Bioscience). BD media (1 L) was added to the large compartment, and the artificial mouse was placed in the incubator. After one week, the cells were removed and centrifuged, and the supernatant containing the mAb was collected and frozen. The cell pellets were then resuspended in BD media with 20% HI-FBS (15 mL) and returned to the small compartment of the artificial mouse; these processes were repeated until cell viability was below 20%.

Purification of mAb CS-35. The collected supernatant was adjusted to pH 7−9 with 1 M Tris buffer (pH 8.0), and ammonium sulfate was added to a final concentration of 50%. The solution was stirred at 4 °C for 2 h and then centrifuged. Resuspension of the pellets in 0.75 M Tris buffer, 0.15 M NaCl, pH 8.0, was followed by addition of ammonium sulfate again to a final concentration of 50%. The solution was stirred at 4 °C for 2 h and then centrifuged. After centrifugation, the pellets were resuspended in 0.05 M Tris buffer, 0.15 M NaCl, pH 8.0, and dialyzed overnight at 4 °C against 2 L of this buffer (pH 8.0). The dialyzed antibody was loaded onto a protein A column using the dialysis buffer, and the mAb was eluted with 0.1 M citric acid buffer (pH 4.0). The eluate was neutralized and dialyzed to obtain the purified mAb as verified by SDS-PAGE (12.5%). The OD value measured by UV spectrometry (A280) was divided by the extinction coefficient for a mAb (1.3) to determine the amount of protein.

Biotinylation of mAb CS-35. Biotinylation of mAb CS-35 was achieved using either a commercially available biotinylation kit (Amersham) or a biotinylating reagent (Pierce). When using the biotinylation kit, 2.5 mg of mAb CS-35 was diluted with 0.04 M sodium

(16) Recent reviews: (a) Dam, T. K.; Brewer, C. F. *Chem. Rev.* **2002**, *102*, 387−489. (b) Gabius, H. J.; Siebert, H. C.; Andre, S.; Jimenez-Barbero, J.; Rudiger, H. *ChemBioChem* **2004**, *5*, 741−764. (c) Collins, B. E.; Paulson, J. C. *Curr. Opin. Chem. Biol.* **2004**, *8*, 617−625. (d) Ambrosi, M.; Cameron, N. R.; Davis, B. G. *Org. Biomol. Chem.* **2005**, *3*, 1593−1608.

(17) (a) Quiocho, F. A. *Pure Appl. Chem.* **1989**, *61*, 1293−1306. (b) Lemieux, R. U. *Acc. Chem. Res.* **1996**, *29*, 373−380.

(18) (a) Nurizzo, D.; Turkenburg, J. P.; Charnock, S. J.; Roberts, S. M.; Dodson, E. J.; McKie, V. A.; Taylor, E. J.; Gilbert, H. J.; Davies, G. J. *Nature Struct. Biol.* **2002**, *9*, 665−668. (b) Hövel, K.; Shallom, D.; Niefind, K.; Belakhov, V.; Shoham, G.; Baasov, T.; Shoham, Y.; Schomburg, D. *EMBO J.* **2003**, *22*, 4922−4932. (c) Miyanaga, A.; Koseki, T.; Matsuzawa, H.; Wakagi, T.; Shoun, H.; Fushinobu, S. *J. Biol. Chem.* **2004**, *279*, 44907−44914. (d) Yamaguchi, A.; Tada, T.; Wada, K.; Nakaniwa, T.; Kitatani, T.; Sogabe, Y.; Takao, M.; Sakai, T.; Nishimura, K. *J. Biochem.* **2005**, *137*, 587−592. (e) Proctor, M. R.; Taylor. E. J.; Nurizzo, D.; Turkenburg, J. P.; Lloyd, R. M.; Vardakou, M.; Davies, G. J.; Gilbert, H. J. *Proc. Natl. Acad. Sci. U. S. A.* **2005**, *102*, 2697−2702. (f) Taylor, E. J.; Smith, N. L.; Turkenburg, J. P.; D'Souza, S.; Gilbert, H. J.; Davies, G. J. *Biochem. J.* **2006**, *395*, 31−37. (g) Miyanaga, A.; Koseki, T.; Matsuzawa, H.; Wakagi, T.; Shoun, H.; Fushinobu, S. *J. Appl. Glycosci.* **2006**, *53*, 143−148.

(19) (a) Nagem, R. A. P.; Rojas, A. L.; Golubev, A. M.; Korneeva, O. S.; Eneyskaya, E. V.; Kulminskaya, A. A.; Neustroev, K. N.; Polikarpov, I. *J. Mol. Biol.* **2004**, *344*, 471−480. (b) Alberto, F.; Bignon, C.; Sulzenbacher, G.; Henrissat, B.; Czjzek, M. *J. Biol. Chem.* **2004**, *279*, 18903−18910. (c) Verhaest, M.; van den Ende, W.; Le Roy, K.; De Ranter, C. J.; van Laere, A.; Rabijns, A. *Plant J.* **2005**, *41*, 400−411. (d) Verhaest, M.; Le Roy, K.; Sansen, S.; de Coninck, B.; Lammens, W.; De Ranter, C. J.; van Laere, A.; van den Ende, W.; Rabijns, A. *Acta Crystallogr., Sect. F: Struct. Biol. Cryst. Commun.* **2005**, *61*, 766−768. (e) Alberto, F.; Jordi, E.; Henrissat, B.; Czjzek, M. *Biochem. J.* **2006**, *395*, 457−462.

(20) (a) Meng, G. Y.; Fütterer, K. *Nature Struct. Biol.* **2003**, *10*, 935−941. (b) Martínez-Fleites, C.; Ortíz-Lombardía, M.; Pons, T.; Tarbouriech, N.; Taylor, E. J.; Arrieta, J. G.; Hernández, L.; Davies, G. J. *Biochem. J.* **2005**, *390*, 19−27.

(21) (a) Casset, F.; Hamelryck, T.; Loris, R.; Brisson, J.-R.; Tellier, C.; Dao-Thi, M.-H.; Wyns, L.; Poortmans, F.; Pérez, S.; Imberty, A. *J. Biol. Chem.* **1995**, *270*, 25619−25628. (b) Loris, R.; Imberty, A.; Beeckmans, S.; Van Driessche, E.; Read, J. S.; Bouckaertt, J.; De Greve, H.; Buts, L.; Wyns, L. *J. Biol. Chem.* **2003**, *278*, 16297−16303.

(22) Forst, D.; Welte, W.; Wacker, T.; Diederichs, K. *Nat. Struct. Biol.* **1998**, *5*, 37−46.

(23) Houseknecht, J. B.; Lowary, T. L.; Hadad, C. M. *J. Phys. Chem. A.* **2003**, *107*, 5763−5777.

(24) (a) D'Souza, F. W.; Lowary, T. L. *Org. Lett.* **2000**, *2*, 1493−1495. (b) D'Souza, F. W.; Ayers, J. D.; McCarren, P. R.; Lowary, T. L. *J. Am. Chem. Soc.* **2000**, *122*, 1251−1260. (c) Yin, H.; D'Souza, F. W.; Lowary, T. L. *J. Org. Chem.* **2002**, *67*, 892−903. (d) Gadikota, R. R.; Callam, C. S.; Wagner, T.; Del Fraino, B.; Lowary, T. L. *J. Am. Chem. Soc.* **2003**, *125*, 4155−4165.

(25) Zhu, X.; Kawatkar, S.; Rao, Y.; Boons, G.-J. *J. Am. Chem. Soc.* **2006**, *128*, 11948−11957.

(26) See Supporting Information for details on preparation.

(27) (a) Crich, D.; Pedersen, C. M.; Bowers, A. A.; Wink, D. J. *J. Org. Chem.* **2006**, *72*, 1553−1565. (b) Nacario, R. C.; Lowary, T. L.; McDonald, R. *Acta Crystallogr., Sect. E: Struct. Rep. Online* **2007**, *63*, o498−o500.

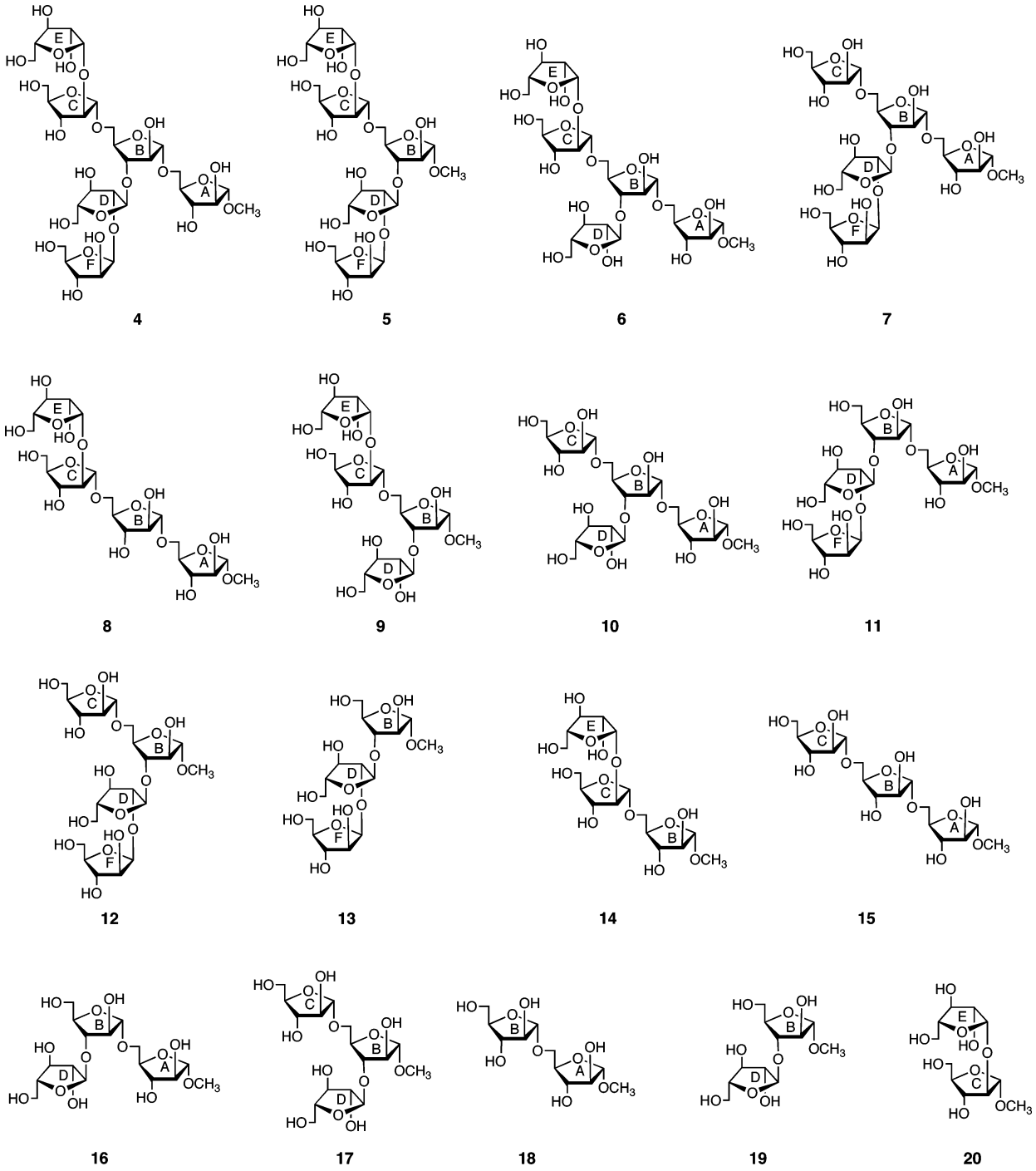

Figure 2. Methyl glycoside derivatives of Ara6 (**4**) and all possible oligosaccharide fragments (**5**−**20**). Rings have been lettered to facilitate comparison with **1** and **2**. Disaccharide **20** also corresponds to the DF fragment of **4**.

bicarbonate (1 mg/mL) before the biotinylation reagent was added. After agitating for 1 h at rt, the biotinylated mAb was purified on a Sephadex G25 column. To biotinylate mAb CS-35 using the Biotin-LC-Hydrazide reagent, cold 0.02 M sodium meta-periodate solution (1 mL) was added to a 2 mg/mL solution of mAb CS-35 in 0.1 M NaOAc buffer, pH 5.5. The oxidation reaction proceeded in the dark for 30 min at 0 °C then glycerol was added to a concentration of 15 mM, and the solution was incubated for an additional 5 min at 0 °C. The reaction mixture was dialyzed overnight against 0.1 M NaOAc buffer, pH 5.5. After dialysis, 0.05 M biotin hydrazide in DMSO was added to a final concentration of 0.005 M, and the reaction was continuously agitated for 2 h at rt. The reaction solution was centrifuged using a Centricon filter with a molecular weight cut off of 10 000 to remove unreacted reagent, and the resulting solution was stored in phosphate buffered saline (PBS) buffer. Biotinylation of the mAb was confirmed by a Western Blot with an anti-biotin antibody.

Preparation of an Affinity Column for Frontal Affinity Chromatography−Mass Spectrometry (FAC−MS) Analysis. Silica capillary tubing (2.5 or 5 cm, 250 μM ID, 360 μM OD) was packed with Streptavidin-CPG (controlled-pore glass) beads (Purebiotech, 37−74 μm), and the biotinylated mAb CS-35 was immobilized by infusion in PBS buffer (pH 7.2, 0.5 mL of an ∼1000 nM solution) onto the column. Any unoccupied sites on the streptavidin were blocked with biotin to prevent nonspecific binding by substrates.

FAC−MS Assay. The FAC−MS system was an integrated module composed of two high-flow-rate precision nanofluidic delivery systems

Scheme 1

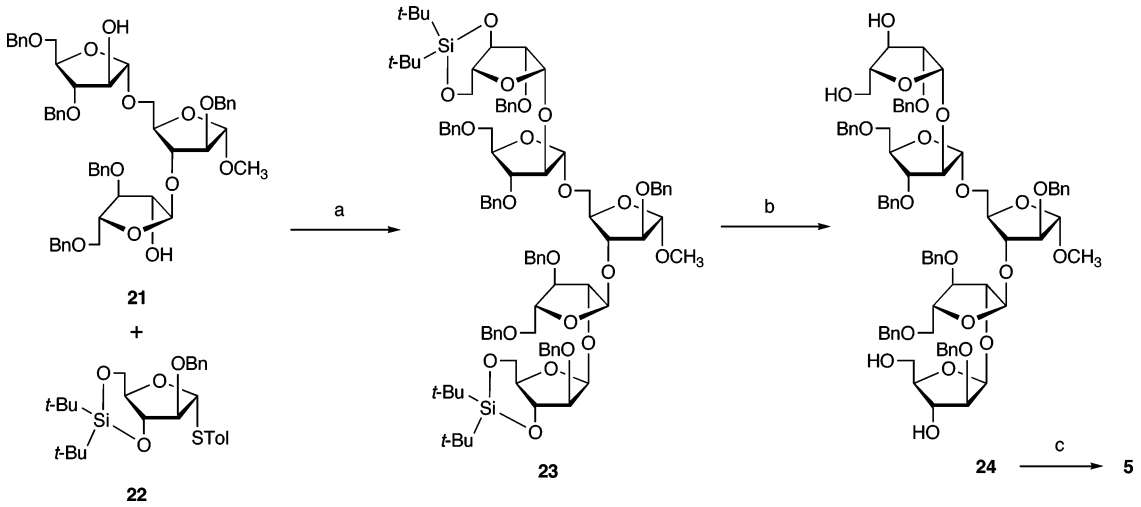

[a] NIS, AgOTf, CH_2Cl_2, −30 °C, 92%. [b] *n*-Bu_4NF, THF, rt, 62%;. [c] H_2, $Pd(OH)_2$/C, rt, 83%.

(Pump A and Pump B) and a six-port valve (Scivex Confluent Nano Fluidic Module, Upchurch).[28] Pump A delivered the eluent buffer, 0.01 M NH_4OAc buffer (pH 7.2), at a flow rate of 1 μL/min through the valve, where compounds were injected. The FAC column was connected from the outlet of the injection valve to a micro tee. A 90% methanol solution was introduced through pump B at a flow rate of 4 μL/min. In online mode, the combined flow was directed into an electrospray mass spectrometer (Agilent 1100 MSD, model A). For characterization of the compound set (quasimolecular ion determination), the spectrometer scanned from 150−1000 *m/z* in positive-ion mode. Elution of compounds from the FAC column was continuously monitored by selected ion monitoring (SIM) of the $(M + Na)^+$ ion for each compound in the mixture, which consisted of four oligosaccharides of different molecular weights. Breakthrough volumes were measured as midpoints in the extracted ion chromatograms. All data were processed with Microsoft Excel software, and association constants were determined as reported previously.[29]

Generation of F_{ab} Fragment. Papain (2.5 mg/mL) was diluted in digestion buffer (50 mM Tris-Cl, pH 8.0 containing 150 mM NaCl, 2 mM EDTA, and 10 mM DTT) and activated for 15 min at 37 °C before addition to CS-35 mAb. F_{ab} fragments were prepared by adding 100 μg the above activated papain into 20 mL of 1 mg/mL mAb in 50 mM Tris-Cl, pH 8.0 containing 150 mM NaCl, 2 mM EDTA, and 5 mM DTT and incubated at room temperature for 1.5 h. The cleavage was stopped by addition of iodoacetamide (final concentration of 25 mM) and incubation of the mixture for 1 h on ice. The mixture was passed over a protein A affinity column, and the F_{ab} fragment was recovered in the load through fraction. The digestion and F_{ab} production were confirmed by SDS-PAGE.

Direct ES−MS Binding Assay. The association constants, K_{assoc}, for F_{ab} binding to ligands **4**−**8** were determined using the *direct* ES−MS technique.[30] These measurements were performed using an Apex II 9.4 T Fourier transform ion cyclotron resonance (FTICR) mass spectrometer (Bruker, Billerica, MA) equipped with a temperature-controlled nanoflow electrospray (nanoES) ion source.[31] The nanoES solutions were prepared from aqueous stock solutions of F_{ab} and ligand with known concentrations. Unless otherwise indicated, aqueous ammonium acetate was added to the nanoES solution to yield a final buffer concentration of 10 mM. NanoES was performed using an aluminosilicate capillary (1.0 mm o.d., 0.68 mm i.d.), pulled to 4−7 μm o.d. at one end using a P-2000 micropipette puller (Sutter Instruments, Novato, CA). The electric field required to spray the solution was established by applying a voltage of +900 V to a platinum wire inserted inside the glass tip. The solution flow rate was typically 20 nL/min. The droplets and gaseous ions produced by nanoES were introduced into the mass spectrometer through a stainless steel capillary (i.d. 0.43 mm) maintained at an external temperature of 66 °C. The ion/gas jet sampled by the capillary (+50 V) was transmitted through a skimmer (−2 V) and stored electrodynamically in an rf hexapole. Unless specified otherwise, a hexapole accumulation time of 2.5 s was used for all experiments. Ions were ejected from the hexapole and accelerated to −2700 V into the superconducting magnet, decelerated, and introduced into the ion cell. The trapping plates of the cell were maintained at a constant potential of +1.6 V throughout the experiment. The typical base pressure for the instrument was $\sim 5 \times 10^{-10}$ mbar. Data acquisition was controlled by an SGI R5000 computer running the Bruker Daltonics XMASS software, version 5.0. Mass spectra were obtained using standard experimental sequences with chirp broadband excitation. The time domain signal, consisting of the sum of 50−100 transients containing 128 K data points per transient, was subjected to one zero-fill prior to Fourier transformation.

The value of K_{assocc} was calculated using eq 1:

$$K_{assoc} = \frac{R}{[L]_o - \frac{R[P]_o}{1+R}} \quad (1)$$

where $[P]_o$ and $[L]_o$ are the initial concentrations of F_{ab} and ligand, respectively and *R* is the ratio of the ion intensity (*I*) of the bound and unbound protein ions (i.e., $I(PL^{n+})/I(P^{n+})$) determined from the mass spectrum. Because ES typically produces P^{n+} and PL^{n+} ions with a distribution of charge states, the *R* value is obtained from the sum of all signal intensities corresponding to ions of the complex divided by the sum of all the signal intensities corresponding to the protein ions over all the observed charge states.[32] When using FTICR MS, for which the ion signal is proportional to the abundance and charge state of the

(28) Ng, E. S. M.; Yang, F.; Kameyama, A.; Palcic, M. M.; Hindsgaul, O.; Schriemer, D. C. *Anal. Chem.* **2005**, *77*, 6125−6133.
(29) (a) Schriemer, D. C.; Bundle, D. R.; Li, L.; Hindsgaul, O. *Angew. Chem., Int. Ed.* **1998**, *37*, 3383−3387. (b) Zhang, B.; Palcic, M. M.; Schriemer, D. C.; Alvarez-Manilla, G.; Pierce, M.; Hindsgaul, O. *Anal. Biochem.* **2001**, *299*, 173−182. (c) Fort, S.; Kim, H.-S.; Hindsgaul, O. *J. Org. Chem.* **2006**, *71*, 7146−7154.
(30) Daniel, J. M.; Friess, S. D.; Rajagopalan, S.; Wendt, S.; Zenobi, R. *Int. J. Mass. Spectrom.* **2002**, *216*, 1−27.
(31) Daneshfar, R.; Kitova, E. N.; Klassen, J. S. *J. Am. Chem. Soc.* **2004**, *126*, 4786−4787.
(32) Wang, W. J.; Kitova, E. N.; Klassen, J. S. *Methods Enzymol.* **2003**, *362*, 376−397.

ions, the measured ion intensities must be normalized for charge state, n, eq 2.[33]

$$R = \frac{\sum_n I(\mathrm{PL})^{n+}/n}{\sum_n I(\mathrm{P})^{n+}/n} \quad (2)$$

Nonspecific binding between protein and carbohydrate, which readily occurs during the nanoES process, will influence the intensities measured for the P^{n+} and PL^{n+} ions.[34] This is particularly problematic when studying weakly binding ligands because relatively high concentrations (>50 μM) of ligand are required to observe abundant specific PL complex. Recently, a method to quantitatively account for the contribution of nonspecific complexes to the nanoES−MS spectra was reported.[34] Briefly, this method involves the addition of a reference protein (P_{ref}) that exhibits no specific binding activity toward the ligands of interest, to the ES solution. The distribution of ligands bound nonspecifically to P_{ref} can be used to correct the measured intensities for the P^{n+} and specific PL^{n+} ions for nonspecific ligand binding. The corrected ion intensities lead to more reliable values of K_{assoc}.

Isothermal Titration Microcalorimetry. All isothermal titration measurements were made using a Microcal VP-ITC titration microcalorimeter.[35] To accurately determine the concentration of CS-35 F_{ab}, purified F_{ab} was equilibrated against Milli-Q water using an Amicon ultracentrifugation unit and lyophilized. The mass of F_{ab} was measure and then dissolved in a 50 mM Tris buffer (pH 7.2) containing 150 mM NaCl to a final concentration of 3.3 mg/mL. The ligands, **4** and **6**, were also lyophilized and dissolved in the same buffer used to equilibrate the CS-35 F_{ab} solution. The calorimeter cell, with a volume of 1.3215 mL, was filled with the CS-35 F_{ab} solution. The ligand was titrated in 35 × 8 μL injections with 6 min intervals between injections. The value of c, which is defined as the product of the binding constant K_{assoc} and the concentration of CS-35 F_{ab}, was ∼2 for all measurements. This value is within the theoretical range of suggested c values, and the ligand concentrations were at least 10 times the concentration of CS-35 F_{ab}, which is recommended to obtain a strong binding isotherm.[36] The results were evaluated with the ORIGIN software package (MicroCal Inc., Northampton, MA) using a single binding-site model.

NMR Spectroscopy. For the purpose of resonance assignments, the lyophilized oligosaccharides were dissolved in D_2O (eurisotope, 99.97%), and TSP (δ = 0.0 ppm) was used as an internal standard. Samples for STD NMR experiments contained F_{ab} fragments of mAb CS-35 at a concentration of 37 μM in 25 mM phosphate buffer at pH 7.0 (7.4 for **7** and **14**). Oligofuranosides were titrated to that solution to a final concentration of 1 mM in 25 mM phosphate buffer pH 7.0 (7.4 for compounds **7** and **14**). Most measurements were done in 3 mm NMR tubes. STD NMR experiments were performed as pseudo-2D experiments at 280 K for weak binders and 310 K for strong binders (for definition of weak/strong binders see Figure 8). A spin lock filter of 35 ms at 6.5 kHz strength was used to suppress the protein background. Residual HDO was suppressed using a W3 Watergate sequence[37] with an interpulse delay of 333 μs resulting in next nulls at 7.7 and 1.7 ppm. Only the anomeric proton of ring A was slightly suppressed by the Watergate sequence. Spectra without suppression of HDO were also recorded to cross check the results (data not shown). The on-resonance frequencies were chosen as +1 ppm or +7 ppm, and the off-resonance frequency was set at +40 ppm. The relaxation delay was 3.8 s plus the respective saturation time. A saturation time of 2.0 s was used for a single point, i.e., one saturation time only, in the epitope mapping. The spectral width was 4 kHz with 32k data points. Control experiments were performed under the same conditions in the absence of F_{ab} fragments to exclude the possibility of direct irradiation of ligand signals. In addition, glucose was added to one sample as a negative control and, as expected, showed no STD signals (see Figure S1 in Supporting Information). For competition experiments, STD NMR spectra were recorded using 256 scans under the same conditions as for experiments used for epitope mapping. Because complete displacement was observed, only one titration step was performed at equal molar amounts of the competing ligand. All spectra were recorded on a Bruker Avance DRX 500 equipped with a TCI cryogenic probe. The number of scans varied depending on the signal-to-noise ratio.

For assignment purposes, we applied standard pulse sequences for DQF-COSY, TOCSY, NOESY, ^{1}H,^{13}C-HSQC, ^{1}H,^{13}C-HMBC, and ^{1}H,^{13}C-HSQC-TOCSY experiments. Additionally, the variable time version of the gradient-enhanced chemical shift selective filtering (ge-CSSF) technique[38] was used. The 1D ge-CSSF-TOCSY and -ROESY versions were applied to facilitate the assignment process and provide an unambiguous peak assignment. Examples of these spectra and tables with full assignments of ^{1}H and ^{13}C resonances in selected oligosaccharides are provided in the Supporting Information (Figures S2−S4, Tables S1, S2). The CSSF increment Δ was set to 4 ms throughout this work, whereas the length of the CSSF t_{max} was adjusted according to the required selectivity of the filter. For saccharides **4**, **6**, and **8**, the assignment was verified at 310 K, as these compounds were used for STD NMR at this particular temperature. The standard inversion recovery pulse sequence was used to determine ^{1}H T_1 relaxation times. Data were analyzed using XWIN-NMR 3.5 (Bruker). ^{13}C T_1 relaxation measurements were performed using the fast-inversion recovery method.[39] Data were fitted using nonlinear least-square fitting algorithm included in Scientific Python.[40] NMR data were processed with NMRPipe[41] and further analyzed with CCPN.[42] High-resolution 1D ge-CSSF-TOCSY experiments were performed in combination with a full line shape analysis in Bruker DAISY[43] to extract accurate $^3J_{HH}$.

PSEUROT Calculations. All calculations were done with PSEUROT 6.3 following modification of the parameters provided in the program for the arabinofuranosyl ring. The electronegativities (in D_2O) used were as follows: 1.25 for OH; 1.26 for OR; 0.68 for CH_2OH; 0.62 for CH(OR); 0.50 for $CH(OR)_2$; and 0.0 for H.[44] For each endocyclic torsion angle, the parameters α and ϵ were set to 1 and 0, respectively. To translate the exocyclic H,H torsion angles (Φ_{HH}) into the endocyclic torsion angles (ν_i) that are used to determine the pseudorotational phase angle (P), the program makes use of the relationship: $\Phi_{H,H} = A\nu_i + B$. The values of A and B used were those previously calculated for the methyl D-arabinofuranosides.[45] In all calculations, the puckering amplitude (Φ_m) for all rings was kept constant at 39°. For the β-D-Ara$f$ rings, an extended Altona-Sundaralingam formula proposed by Diez et al.[46] was used to correct for the minor inaccuracies in the representation of non-equilateral puckered rings. The Diez parameters

(33) Wang, W. J.; Kitova, E. N.; Klassen, J. S. *Anal. Chem.* **2003**, *75*, 4945−4955.
(34) Sun, J. X.; Kitova, E. N.; Wang, W. J.; Klassen, J. S. *Anal. Chem.* **2006**, *78*, 3010−3018.
(35) (a) Bundle, D. R.; Alibes, R.; Nilar, S.; Otter, A.; Warwas, M.; Zhang, P. *J. Am. Chem. Soc.* **1998**, *120*, 5317−5318. (b) Chervenak, M.; Toone, E. J. *J. Am. Chem. Soc.* **1994**, *116*, 10533−10539.
(36) Christensen, T.; Toone, E. J. *Methods Enzymol.* **2003**, *362*, 486−504.
(37) Piotto, M.; Saudek, V.; Sklenář, V. *J. Biomol. NMR* **1992**, *2*, 661−665.
(38) Robinson, P. T.; Pham, T. N.; Uhrin, D. *J. Magn. Reson.* **2004**, *170*, 97−103.
(39) Canet, D.; Levy, G. C.; Peat, I. R. *J. Magn. Reson.* **1975**, *18*, 199−204.
(40) Jones, E.; Oliphant, T.; Peterson, P. *SciPy: Open Source Scientific Tools for Python*; 2001.
(41) Delaglio, F.; Grzesiek, S.; Vuister, G. W.; Zhu, G.; Pfeifer, J.; Bax, A. *J. Biomol. NMR* **1995**, *6*, 277−293.
(42) Vranken, W. F.; Boucher, W.; Stevens, T. J.; Fogh, R. H.; Pajon, A.; Llinas, M.; Ulrich, E. L.; Markley, J. L.; Ionides, J.; Laue, E. D. *Proteins* **2005**, *59*, 687−696.
(43) *DAISY software package*, part of TopSpin 2.0pl4 Bruker BioSpin GmbH; 2006.
(44) Altona, C.; Francke, R.; de Haan, R.; Ippel, J. H.; Daalmans, G. J.; Westra Hoekzema, A. J. A.; van Wijk, J. *Magn. Reson. Chem.* **1994**, *32*, 670−678.
(45) Houseknecht, J. B.; Altona, C.; Hadad, C. M.; Lowary, T. L. *J. Org. Chem.* **2002**, *67*, 4647−4651.

Table 1. Thermodynamic Parameters of Oligosaccharides **4**−**8** for CS-35 by FAC−MS, ES−MS, and ITC at 25 °C[a,b]

oligosaccharide	K_{assoc} (M^{-1}) (FAC–MS)	K_{assoc} (M^{-1}) (ES–MS)	K_{assoc} (M^{-1}) (ITC)	$-\Delta H_{assoc}$ (kcal mol^{-1}) (ES–MS)	$-\Delta H_{assoc}$ (kcal mol^{-1}) (ITC)
4	1×10^5	$1.6 \pm 0.2 \times 10^5$	$1.7 \pm 0.2 \times 10^5$	21.7 ± 0.1	15.3 ± 0.4
5	Not tested	$3.4 \pm 0.6 \times 10^2$	Not tested	Not tested	Not tested
6	8×10^4	$9.9 \pm 0.5 \times 10^4$	$9 \pm 1 \times 10^4$	21.4 ± 0.5	15 ± 1
7	NB[c]	$6.2 \pm 0.7 \times 10^3$	Not tested	11.1 ± 0.3	Not tested
8	2×10^4	$2.6 \pm 0.1 \times 10^4$	Not tested	19 ± 1	Not tested

[a] Error corresponds to one standard deviation. [b] FAC−MS experiments were carried out using full-length antibody, whereas the ES−MS measurements were done using the F_{ab} fragment. K_{assoc} values obtained from FAC−MS and ITC measurements have been corrected to take into account the effect of the extra binding site possessed by the mAb compared to the F_{ab}. [c] NB = no binding detected.

(α_i, ϵ_i) used were (1.0136, 0.33) for ϕ_4, (1.0221, −0.24) for ϕ_0, and (0.9966, −1.29) for ϕ_1.[47] The endocyclic torsion angles ϕ_0, ϕ_1, and ϕ_4 were as previously defined (see Figure S7 in the Supporting Information).[45]

Results

FAC−MS. As an initial screen to determine ligand affinity for mAb CS-35, oligosaccharides **4** and **6**−**20** were evaluated using FAC−MS. This technique is a rapid method for determining the affinity of a ligand, or set of ligands, for a receptor and has been used previously to map the combining sites of carbohydrate-binding antibodies, lectins, and enzymes.[28,29] Mixtures containing four oligosaccharides of different molecular weight were analyzed, and only three of the 17 oligosaccharides shown in Figure 2 were bound by the protein. In agreement with an earlier study,[15] hexasaccharide **4** and tetrasaccharide **8** were ligands. Also consistent with previous studies, tetrasaccharide **11**, which lacks both residues C and E, did not bind to the mAb. This screen also identified that pentasaccharide **6**, which lacks one of the β-Ara*f* residues (F), is bound by the antibody. Pentasaccharide **7**, which, compared to the hexasaccharide, lacks the other β-Ara*f* residue (E), did not bind, thus demonstrating the importance of residue E in the recognition of mycobacterial arabinans by CS-35. These results point to an extended combining site requiring, at a minimum, a tetrasaccharide epitope (residues A, B, C, and E). Determination of K_{assoc} for **4**, **6**, and **8** using the FAC−MS method (Table 1) indicated that hexasaccharide **4** and pentasaccharide **6** bind with comparable affinity ($\sim 10^5$ M^{-1}), whereas the strength of the interaction with tetrasaccharide **8** is lower.

ES−MS and Microcalorimetry. To gain a more precise measure of the ligand binding affinities, the direct ES−MS assay was used to measure the K_{assoc} values for the CS-35 F_{ab} fragment with ligands **4**−**8** over a temperature range of 20−37 °C. Use of the full-length antibody in the ES−MS studies was complicated by the glycosylation of the F_c moiety. The presence of numerous glycoforms, all of different molecular weights, led to complex mass spectra that could not be unambiguously analyzed. Thus, the F_{ab} fragment, obtained by treatment of the antibody with papain, was used in these ES−MS investigations.

Illustrative nanoES mass spectra for aqueous solutions of CS-35 F_{ab}, in the absence and presence of hexasaccharide **4** and P_{ref}, are given in Figure 3. As can be seen in Figure 3a, digestion of the mAb with papain led to a heterogeneous mixture of F_{ab} species, a result that has been observed in other antibody digestions using papain.[48] Four distinct F_{ab} species, **a**, **b**, **c**, and **d**, with masses of 48.25 (**a**), 47.90 (**b**), 48.92 (**c**), and 49.23 kDa (**d**), respectively, were detected at charge states ranging from +13 to +15. In the presence of **4**, the F_{ab}^{n+} and $(F_{ab} + \mathbf{4})^{n+}$ ions are clearly resolved in the mass spectrum (Figure 3b). Notably, only unbound P_{ref} ions are detected, indicating that nonspecific ligand binding did not contribute to the mass spectrum. In calculating the K_{assoc} values, the measured ion intensities of all the observed F_{ab} species and their complexes with ligand were added together to obtain values for $I(P^{n+})$ and $I(PL^{n+})$, respectively. The K_{assoc} values obtained for ligands **4**−**8** at 25 °C are given in Table 1.

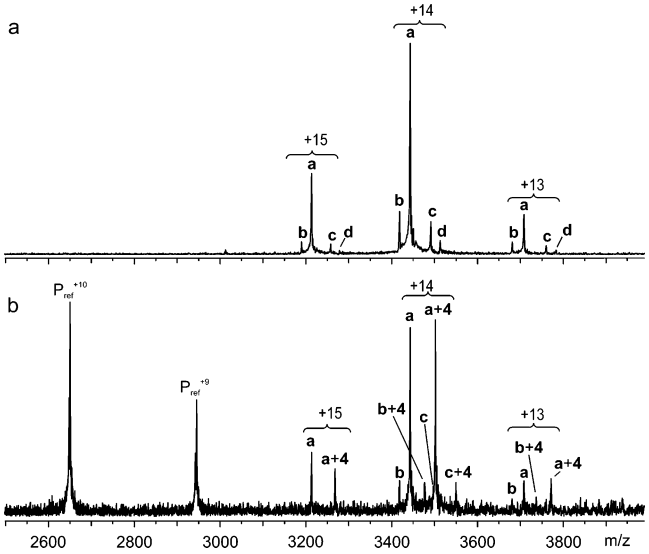

Figure 3. NanoES mass spectra obtained in positive ion mode for an aqueous solution of (a) CS-35 F_{ab} at a concentration of 12 μM and (b) a mixture containing 8 μM CS-35 F_{ab}, 11 μM **4**, and 5 μM of P_{ref} to quantify the nonspecific contributions to the binding constant. All solutions contained 10 mM ammonium acetate (pH 7.2).

The K_{assoc} values determined for **4**, **6**, and **8** are, on average, within 20% of the estimated values obtained by FAC−MS. The low binding affinity of **7**, as determined by nanoES−MS, explains why no binding was detected for this ligand in the FAC−MS study. Thermodynamic parameters for binding of F_{ab} with **4** and **6** at 25 °C were also evaluated using ITC. Importantly, the K_{assoc} values determined by ITC are in excellent agreement with the values determined by ES−MS. The binding affinities for ligands **5** and **7** are much weaker, by a factor of 300 and 30, respectively, compared to **4**. These results confirm the importance of residues A and E in conferring binding specificity.

(46) (a) Diez, E.; Esteban, A. L.; Guilleme, J.; Bermejo, F. L. *J. Mol. Struct.* **1981**, *70*, 61−64. (b) Diez, E.; Esteban, A. L.; Bermejo, F. J.; Altona, C.; de Leeuw, F. A. A. M. *J. Mol. Struct.* **1984**, *125*, 49−65. (c) de Leeuw, F. A. A. M.; van Kampen, P. N.; Altona, C. E.; Diez, E.; Esteban, A. L. *J. Mol. Struct.* **1984**, *125*, 67−88.

(47) Altona, C.; van Wijk, J.; Hassnoot, K.; de Leeuw, F.; Huckriede, D. *PSEUROT 6.2 Manual*; 1995; p 35.

(48) Bennett, K. L.; Smith, S. V.; Truscott, R. J. W.; Sheil, M. M. *Anal. Biochem.* **1997**, *245*, 17−27.

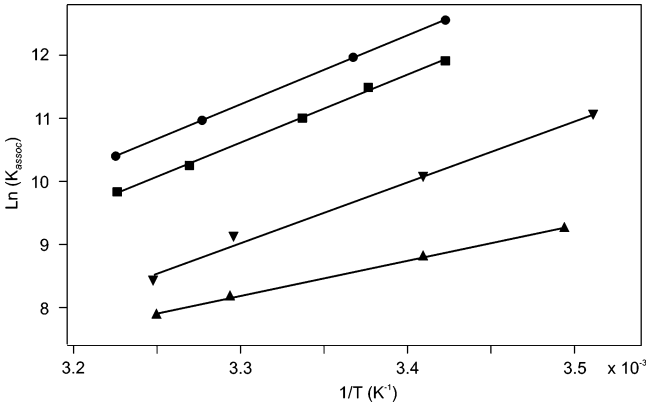

Figure 4. Linear van't Hoff plots constructed from K_{assoc} values obtained from nanoES−MS measurements at varying temperatures for the association of CS-35 F_{ab} with (●) **4**, (■) **6**, (▲) **7**, and (▼) **8**.

Temperature-controlled nanoES−MS has recently been used to estimate ΔH_{assoc} and ΔS_{assoc} values for protein−carbohydrate binding.[31] This approach could not be used for **5** because of the absence of detectable (F_{ab} + **5**) complex at elevated temperatures. However, this technique was used to evaluate the thermodynamic parameters for CS-35 binding to **4**, **6**, **7**, and **8** by measuring their respective K_{assoc} values over a temperature range of 20−37 °C. The temperature dependence of K_{assoc} was modeled using the linear form of the van't Hoff equation, which assumes a constant heat capacity over the temperature range. The van't Hoff plots for each ligand are given in Figure 4. The resultant thermodynamic data obtained from the van't Hoff plots, along with values obtained from ITC measurements are summarized in Table 1.

As can be seen from the data in Table 1, the $-\Delta H_{assoc}$ values for CS-35 F_{ab} binding to **4** and **6** were similar (∼20−21 kcal mol^{-1}). The $-\Delta H_{assoc}$ of binding for **8** was ∼2 kcal mol^{-1} smaller and **7** exhibited the smallest $-\Delta H_{assoc}$, ∼10 kcal mol^{-1} lower compared to **4** and **6**. Thus, the trend in $-\Delta H_{assoc}$ follows the trend in K_{assoc} (and $-\Delta G_{assoc}$). The ΔH_{assoc} value for **4** and **6** interacting with CS-35 F_{ab} were also assessed by ITC. Interestingly, the ΔH_{assoc} values obtained from the linear treatment of K_{assoc} values differed significantly with the values obtained from ITC. The difference in the ΔH_{assoc} values could arise, in part, from the use of the linear form of the van't Hoff equation to analyze the ES−MS derived data. As can be seen in Figure 4, however, the data exhibited excellent linearity for all ligands studied. This discrepancy may arise from the low value of the *c* constant (∼2) in the ITC experiments. Recent work has suggested that binding isotherms with a low *c* value (<10) yield reliable K_{assoc} values but that the ΔH_{assoc} values can be unreliable.[49] Additional support for this explanation is found in the agreement between the K_{assoc} determined at 30 °C by ITC ($7.7 \pm 0.3 \times 10^4$ M^{-1}) and the value predicted by the van't Hoff plot ($7.5 \pm 0.2 \times 10^4$ M^{-1}). This suggests that the temperature-controlled ES−MS technique provides an accurate measure of the temperature dependence of the binding constants and thus yields reliable thermodynamic parameters. It is also worth noting that despite the discrepancies in the absolute values, both methods suggest similar $-\Delta H_{assoc}$ values for **4** and **6** binding to the F_{ab}.

(49) Turnbull, W. B.; Daranas, A. H. *J. Am. Chem. Soc.* **2003**, *125*, 14859−14866.

Assignment of ^{1}H and ^{13}C NMR Spectra and Measurement of $^3J_{HH}$ and ^{13}C T_1 Values. For the assignment of the hexasaccharide and fragments thereof, we followed a fragment-based approach making use of the structural reporter group concept originally developed by Vliegenthart and co-workers.[50] On the basis of previous studies,[51] for the assignment of the hydroxymethyl group protons, H5S and H5R, H5, and H5′, respectively, H5R is assumed to be more upfield than H5S. Starting points for the assignments were the disaccharides that contained the "isolated" furanosidic ring systems (**18**−**20**, Figure 2). Given that all 17 oligosaccharides all contain only D-Ara*f*, there was significant spectral overlap and fully assigning all resonances was challenging. However, by applying homo- and heteronuclear correlation NMR spectroscopy we succeeded in assigning all of the ^{1}H and ^{13}C NMR resonances. Tables with this data can be found in the Supporting Information (Tables S1 and S2). For the analysis of J_{HH} coupling constants, gradient-enhanced chemical shift selective filtered experiments in combination with 1D-TOCSY turned out to be very valuable. Simulation of the corresponding one-dimensional ^{1}H NMR spectra of the individual furanose rings with DAISY[43] yielded a complete set of scalar coupling constants for **4**, **6**−**8**, and **11** (Table S3 in the Supporting Information). The overall quality of the data obtained can be seen from an expansion of the ^{1}H,^{13}C HSQC spectrum of hexasaccharide **4** (Figure 5).

To assess the relative flexibility of the individual furanose rings, we determined ^{13}C spin lattice relaxation times (T_1) for oligosaccharides **4**, **6**−**8**, and **11** as this data is a reasonable probe for molecules of this size.[52] The resulting average NT_1 values[53] of all carbons in each ring (with *N* being the number of protons attached to a particular carbon atom) are summarized in Table 2. The NT_1 values for each carbon in **4**, **6**−**8**, and **11** can be found in the Supporting Information (Table S4). These average NT_1 values suggest that the most mobile residue is A, as might be expected given its location at the reducing terminus of the oligosaccharide. In addition, the terminal β-Ara*f* residues, E and F, appear to be more mobile than the internal residues (B, C, and D). These trends are consistent with available data for other oligosaccharides.[54] The lower average T_1 times for E and F relative to A may be the result of the inherently more rigid nature of β-Ara*f* rings compared to their α-Ara*f* counterparts.[23,55]

With regard to the internal residues, the average T_1 times of the carbons in residue B are significantly lower when glycosylated at both O3 and O5 (**4**, **6**, and **7**) as opposed to when substituted only at one of these positions (**8** and **11**). This suggests that mobility in residue B is lost upon glycosylation, as would be expected. In a similar manner, these T_1 times suggest that residues C and D become less mobile when glycosylated at O2 with residues E and F, respectively. For example, the average T_1 values for residue D in molecules where residue F is attached to O2 (**4**, **7**, and **11**) are approximately

(50) Vliegenthart, J. F. G.; Dorland, L.; van Halbeek, H. *Adv. Carbohydr. Chem. Biochem.* **1983**, *41*, 209−374.
(51) Serianni, A. S.; Barker, R. *Can. J. Chem.* **1979**, *57*, 3160−3167.
(52) LaPlante, S. R. *Curr. Top Chem* **2007**, *272*, 259−296.
(53) Thogersen, H.; Lemieux, R. U.; Bock, K.; Meyer, B. *Can. J. Chem.* **1982**, *60*, 44−57.
(54) (a) Paulsen, H.; Peters, T.; Sinnwell, V.; Lebuhn, R.; Meyer, B. *Liebigs Ann. Chem.* **1984**, 951−976. (b) Paulsen, H.; Peters, T.; Sinnwell, V.; Lebuhn, R.; Meyer, B. *Liebigs Ann. Chem.* **1985**, 489−509.
(55) (a) Gordon, M. T.; Lowary, T. L.; Hadad, C. M. *J. Am. Chem. Soc.* **1999**, *121*, 9682−9692. (b) Gordon, M. T.; Lowary, T. L.; Hadad, C. M. *J. Org. Chem.* **2000**, *65*, 4954−4963.

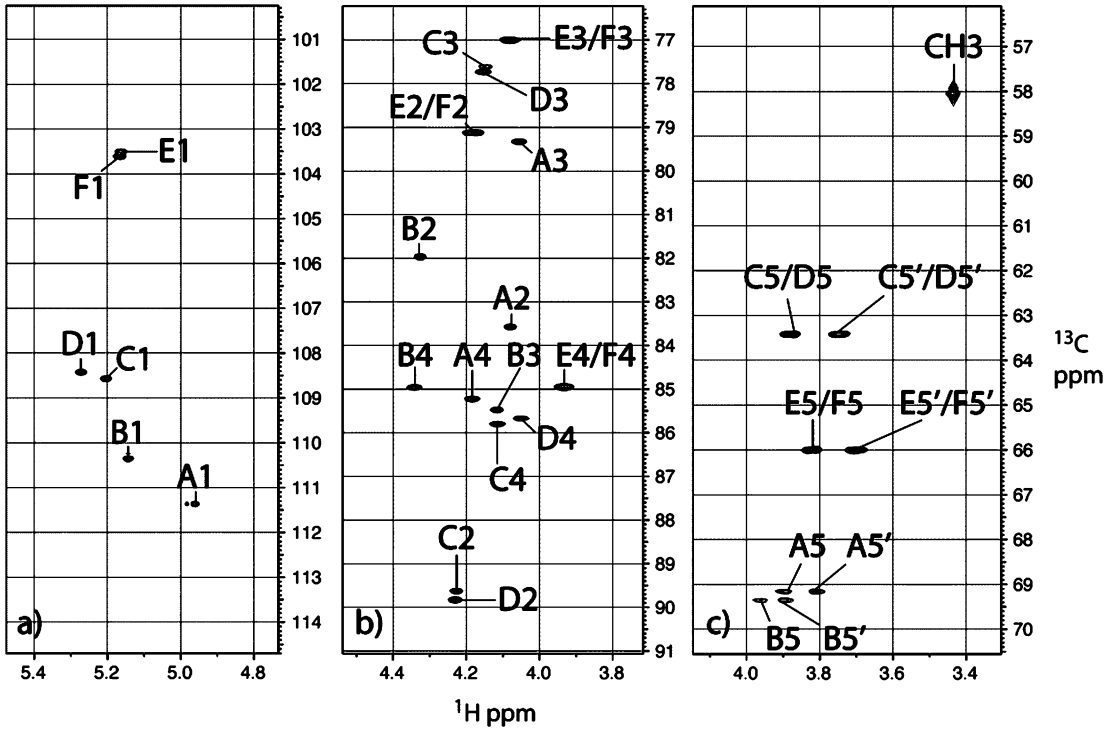

Figure 5. ^{1}H, ^{13}C HSQC spectrum of hexasaccharide **4**. (a) Expansion of the anomeric region (b) and (c) ring proton region. The spectrum was recorded at 280 K with 1024 data points in F2 and 2048 in F1 on a Bruker Avance 500 MHz NMR equipped with a cryogenic probe. Nomenclature used for protons: E1 = H1 of unit E, etc.

Table 2. Average NT_1 Values for **4**, **6**−**8**, and **11**[a]

ring	4	6	7	8	11
A	0.362	0.346	0.357	0.376	0.389
B	0.262	0.333	0.310	0.346	0.446
C	0.305	0.310	0.364	0.366	–
D	0.299	0.363	0.312	–	0.303
E	0.339	0.358	–	0.366	–
F	0.343	–	0.343	–	0.340

[a] In seconds.

0.305 s, whereas in **6**, where residue F is absent, the average T_1 increases to 0.358 s.

We further probed the flexibility of these residues by carrying out PSEUROT[56] calculations using the $^{3}J_{HH}$ obtained by DAISY simulation of the 1D geCSSF-TOCSY spectra. The PSEUROT method assumes that each furanose ring adopts an equilibrium between two low-energy conformers, termed the North (N) and South (S) conformers depending upon their location within the northern or southern hemisphere of the pseudorotational itinerary (Figure 6).[57] The analysis provides the identities of the two conformers (and their populations) that best fit the experimental $^{3}J_{HH}$ data, which is done by the correlation of the coupling constants, through a generalized Karplus equation,[44] with exocyclic H−C−C−H dihedral angles. The coupling constants used in these calculations are provided in the Supporting Information (Table S3), and the results of the PSEUROT analyses are given in Table 3.

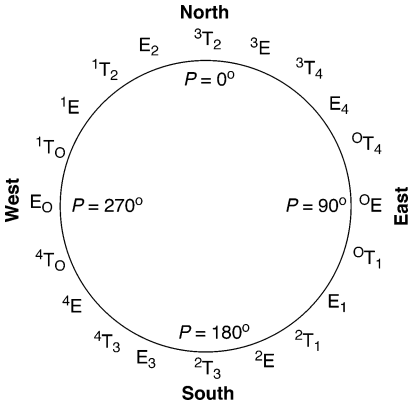

Figure 6. Pseudorotational itinerary for a D-aldofuranose ring.

As in previous studies on D-Ara*f*-containing oligosaccharides,[45,55b,58] these PSEUROT analyses demonstrate that for the α-Ara*f* rings (A, B, C, and D), the rings adopt N conformers in a narrow range of *P* values (46−66°) and that the S conformers are dispersed over a slightly broader range (108−134°). For all but one of the rings, significant populations of each conformer are present. The only α-Ara*f* residue that does not conform to these patterns is ring A of **11**, in which the equilibrium is heavily biased to the S conformer (X_S = 88%), suggesting that the ring adopts essentially a single conformation. The S conformer of this ring is in the same range as that for the other α-Ara*f* residues (P = 118°), however the N conformer differs significantly (P = 328°). We do not, at present, understand why the conformational equilibrium of this ring differs so substantially from the others.

In agreement with the T_1 values measured above, substitution of the other α-Ara*f* rings rigidifies them to some degree. For

(56) (a) van Wijk, J.; Haasnoot, C. A. G.; de Leeuw, F. A. A. M.; Huckriede, B. D.; Westra Hoekzema, A.; Altona, C. *PSEUROT 6.2*; Leiden Institute of Chemistry, Leiden University, 1993; van Wijk, J.; Haasnoot, C. A. G.; de Leeuw, F. A. A. M.; Huckriede, B. D.; Westra Hoekzema, A.; Altona, C. *PSEUROT 6.3*; Leiden Institute of Chemistry, Leiden University, 1999. (b) de Leeuw, F. A. A. M.; Altona, C. *J. Comput. Chem.* **1983**, *4*, 428−437. (c) Altona, C. *Recl. Trav. Chem. Pays-Bas* **1982**, *101*, 413−433.

(57) Altona, C.; Sundaralingam, M. *J. Am. Chem. Soc.* **1972**, *94*, 8205−8212.

(58) Houseknecht, J. B.; Lowary, T. L. *J. Org. Chem.* **2002**, *67*, 4150−4164.

Table 3. PSEUROT Analysis of Arabinofuranose Rings in **4**, **6**−**7**, and **11**[a]

compound	ring[b]	P_N (°)[c]	X_N (%)	P_S (°)[c]	X_S (%)	rms (Hz)
4	A	46	42	128	58	0.0
	B	64	29	124	71	0.0
	C	49	55	113	45	0.0
	D	53	65	113	35	0.0
	E	21	85	184	15	0.33
	F	20	84	184	16	0.45
6	A	47	44	128	56	0.0
	B	59	30	118	70	0.0
	C	44	50	108	50	0.0
	D	51	46	125	54	0.0
	E	22	85	184	15	0.25
7	A	47	44	128	56	0.0
	B	66	32	126	68	0.0
	C	52	41	119	59	0.0
	D	53	63	116	37	0.0
	F	19	85	184	15	0.38
8	A	50	43	134	57	0.0
	B	49	44	123	56	0.0
	C	50	57	113	43	0.0
	E	19	85	184	15	0.38
11	A	328	12	118	88	0.0
	B	49	43	121	57	0.0
	D	52	64	122	36	0.0
	F	20	84	184	16	0.35

[a] Calculated using a constant $\phi_m = 39°$ for all Ara*f* rings. [b] See Figure 2 for ring lettering. [c] P = pseudorotational phase angle.

example, when residue B carries additional sugar residues at both O3 and O5, the ring conformer populations are biased to the S structure: for **4**, the N:S ratio is 29:71 whereas for rings substituted only at O3 or O5 an ∼1:1 N:S ratio is observed (compare **4**, **8**, and **11**). Similar trends are seen for residue D upon glycosylation with F (compare **4**, **7**, and **11** with **6**). In the case of ring C, substitution with residue E leads to a less clear trend but appears to change the bias from S-favored (**7**) to slightly N-favored (**4** and **8**) or, in one case, to a 50:50 conformer mixture (**6**).

For the β-Ara*f* rings (E and F), the equilibria between the N and S conformers is heavily biased to the north with $P_N \approx 19-22°$ and is essentially identical for all compounds. This data is consistent with the NT_1 values (Table 2), which indicated these residues are relatively rigid.

Relative Binding Epitopes from STD Effects. Having fully assigned the spectra of the oligosaccharides and probed their conformational dynamics, STD effects were measured to further probe the bound complex. These experiments were done with a saturation time of 2 s and an on-resonance frequency of +1 ppm. STD spectra of **4** are shown in Figure 7. The corresponding epitopes for oligosaccharides **4**−**8**, **11**, and **14** are summarized in Figure 8 with the relative intensity of the interactions color-coded.

Consistent with the FAC−MS and ES−MS results, analysis of the NMR data shows that the strong binders (**4**, **6**, and **8**) have a common recognition motif containing residues A, B, C and E. Loss of either of the terminal residues, A or E, from this sequence leads to a weaker binding ligand (i.e., loss of residue A from hexasaccharide **4** yields pentasaccharide **5** whereas loss of residue E from **4** affords pentasaccharide **7**).

A second feature that emerges from a comparison of the epitopes in Figure 8 is that as long as residue C is present in the oligosaccharide (**4**−**8**), the overall binding mode is conserved. However, in ligands lacking this residue, e.g., **11**, a tetrasaccharide that contains residues A, B, D, and F, the binding mode appears altered. In oligosaccharides **4**−**8**, the bulk of the saturation transfer is to residues A, B, C, and E, with little to residues D and F. In contrast, in tetrasaccharide **11** the absence of residue C (and as a consequence E) appears to direct the saccharide into the binding pocket such that residue F receives the most substantial saturation transfer. These observations may indicate that the F_{ab} fragment can bind to different portions of the hexasaccharide albeit with different affinities. In the preferred "native" mode, the binding pocket is filled with residues A, B, C, and E, whereas in the second, lower-affinity mode, the binding occurs through residues A, B, D, and F (Figure 9). When presented with tetrasaccharide **11**, which lacks residues C (and E), binding with CS-35 occurs through this low-affinity mode.

We were concerned that the STD signals observed with **11** was due to weak nonspecific binding of the ligand to a region of the protein other than the combining site. Thus, a competition experiment was done, in which **11** was added to the CS-35 F_{ab} and an STD spectrum was recorded. Next, the stronger binding ligand **8** was titrated to the solution to a concentration of 0.5 mM and a second STD spectrum was recorded. Although there is severe spectral overlap in the resonances for these two ligands, the signal for one hydrogen of residue B is sufficiently well resolved between the two compounds and this was used as a diagnostic marker. As shown in the Supporting Information (Figure S5), upon the addition of **8**, to a solution of the **11** and the F_{ab}, the signals for the weaker binding ligand disappeared, strongly suggesting that the two compounds bind to the same site on the protein.

A final trend that emerges is that loss of residue D, though not significantly affecting the binding epitope, markedly changes the K_{assoc}. Both **6** and **8** show very similar STD patterns (Figure 8), but their affinity to the protein differs by 4-fold (Table 1), with pentasaccharide **6** being the better ligand. This increase in affinity appears not to be due to the formation of additional protein contacts with the ligand, as only weak interactions with residue D were detected in STD studies with **6** (Figure 8). Instead, we propose that unit D stabilizes the bound conformation of the ABCE motif but does not contribute to the binding directly. In other words, the presence of a rigid core consisting of residues B, C, and D, leads to higher-affinity binding, provided that residues A and E are also in place. This correlates well with the observation that NOEs for the terminal residues A and E/F in **4** are positive, whereas the central residues B, C, and D display negative NOEs at 500 MHz and 278 K, indicating slower overall motion.

Characterization of the Binding Pocket based on STD Curves. To qualitatively estimate the contribution of aromatic and aliphatic amino acid side chains to the binding, we acquired STD curves for tetrasaccharides **8** and **11**, which represent the two proposed binding modes. For each ligand, two sets of STD experiments were performed, one with the on-resonance frequency set at +1 ppm, the other set with the on-resonance frequency at +7 ppm. Using this approach, the saturation transfer resulting from aromatic protons may be discriminated from saturation transfer resulting from aliphatic protons. It is expected that at +7 ppm the aromatic protons of the F_{ab} fragment contribute more to the saturation transfer as they are

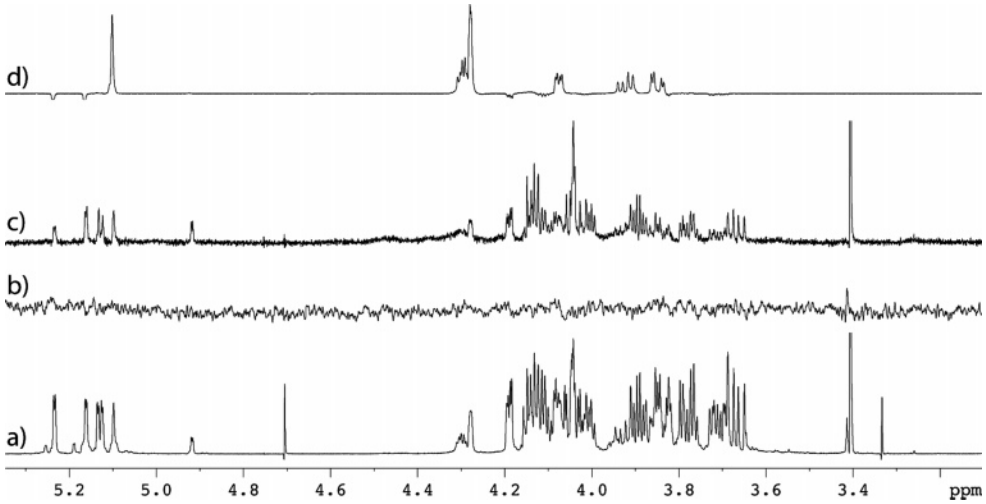

Figure 7. STD NMR spectra of hexasaccharide **4.** (a) Reference spectrum, (b) STD spectrum of **4** in absence of F_{ab} fragment, (c) STD spectrum of **4** in presence of F_{ab}, and (d) 1D geCSSF-TOCSY spectrum of **4** employing selective excitation of unit B.

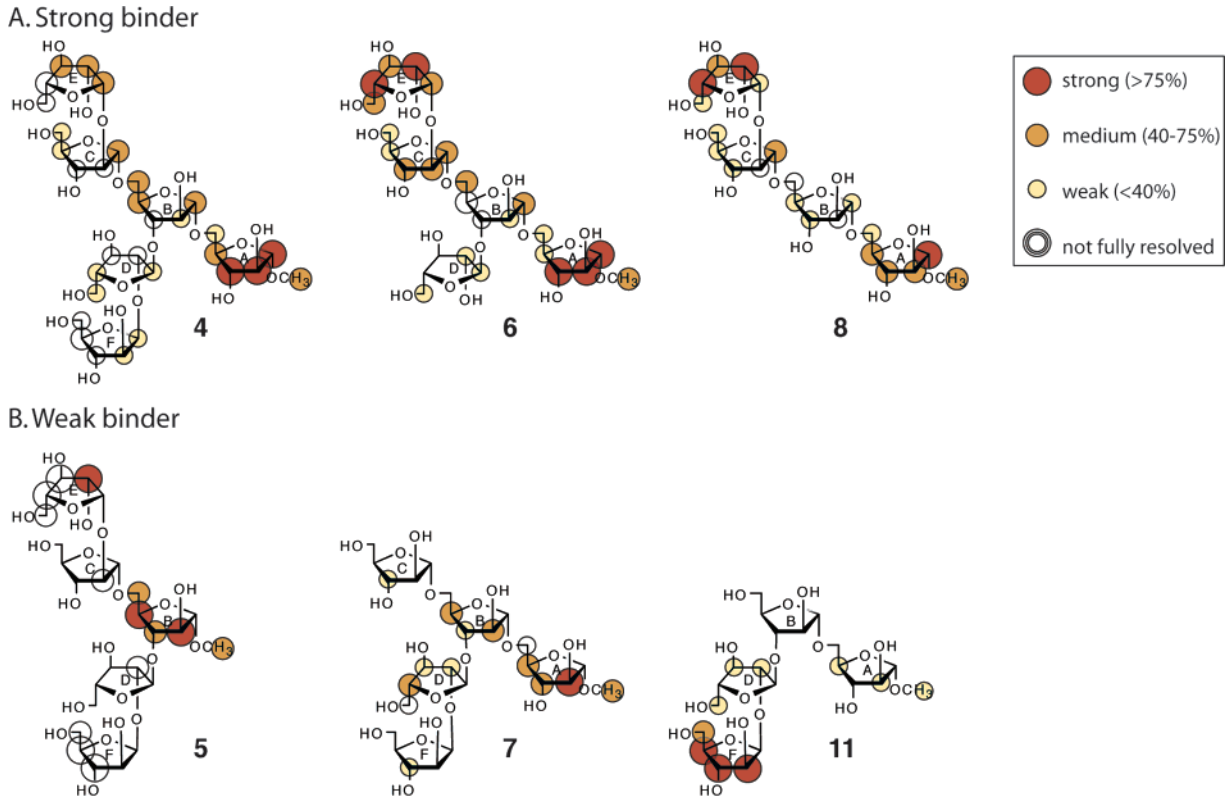

Figure 8. Binding epitopes of oligosaccharides **4**−**8**, **11**, and **14**. Relative binding epitopes are color-coded to indicate strong, medium, or weak STD effects with the protein. STDs that are not fully resolved are colorless with the size of the circle indicating the putative STD strength. It can be seen that residues A and E must be present to allow for proper recognition by the F_{ab} fragment and for the compound to be a strong binder. Note that although tetrasaccharide **11** (containing residues A, B, D, and F) formally has the same length as the "natural" recognition motif, tetrasaccharide **8** (residues A, B, D, and E), it is a significantly weaker ligand as the different glycosidic linkages force the terminal furanose residues into different relative positions. The K_{assoc} of oligosaccharides **4**−**8** and **11** can be found in Table 1.

saturated directly in this case. Similarly, in the experiment in which +1 ppm is the on-resonance frequency greater saturation transfer to ligand will occur if bound in an aliphatic pocket. The STD curves and corresponding tables are found in the Supporting Information (Table S5 and Figure S6). A very efficient way of comparing the data is to subtract the STDs with an on-resonance frequency of +1 ppm from the ones at +7 ppm. If saturation transfer from aromatic protons prevails, a negative value will be expected. The linear initial slope of the STD curves was used to reduce and quantify the experimental error.

For tetrasaccharide **8**, it is observed that initial slope differences of unit E are positive, whereas all other protons deliver negative values. This suggests that CS-35 binds residue E of **8** in a pocket containing predominantly aliphatic amino acid side chains whereas for residues A, B and C the protein contacts are predominantly with aromatic amino acids. In similar experiments with tetrasaccharide **11**, the STD signals to residues

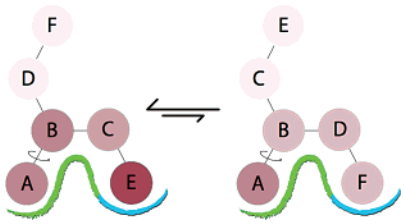

Figure 9. Possible binding modes as deduced from group epitope mapping with STD NMR. (Left) "Natural" binding mode with units A and E making closest contact with protons in the binding site. (Right) Low-affinity alternate binding mode of the ABDF motif. Color code of sub-binding pockets: green = aromatic, blue = aliphatic.

A, B, and D were rather weak, and only STD signals for protons A2, D2, and D4 were detected. However, strong STD signals were seen for residue F and like **11**, this moiety is bound in an aliphatic pocket. These results provide additional support for the model proposed in Figure 9 in that the β-(1→2)-linked Ara*f* residue (E in **8** and F in **6**) appear to both be bound in a pocket containing aliphatic amino acids.

Discussion

Arabinofuranose residues are key constituents of cell wall polysaccharides in mycobacteria and the enzymes involved in arabinan biosynthesis have attracted significant recent attention as targets for new drugs that can be used for the treatment of tuberculosis and other mycobacterial diseases.[4,5] This interest has in turn led to increased research into the basic biochemistry of mycobacterial polysaccharide assembly,[6−8] and a key reagent in these studies has been a monoclonal antibody, CS-35, which was generated against *M. leprae* LAM, but which also binds to LAM from other mycobacterial species as well as AG.[15] In addition, recent work has suggested that antibodies directed toward mycobacterial LAM motifs have potential as anti-tuberculosis vaccines[59] and that detection of anti-LAM antibodies in serum has potential in diagnosing infection by *M. tuberculosis*.[60]

Earlier work using ELISA suggested that the preferred ligand for CS-35 is a hexasaccharide motif (**1**, Figure 1) found at the non-reducing ends of both AG and LAM and that a tetrasaccharide motif (**2**) is also recognized.[15] Beyond those investigations, little is known about the fine ligand specificity of this antibody. A more in-depth understanding of this interaction is important for the use of CS-35 as a bioanalytical tool and in determining epitopes for the preparation of neoglycoconjugate vaccines. Furthermore, complexes between proteins and oligofuranosides are, in general, poorly understood and we view this to be an ideal system for probing such interactions. Our efforts to obtain a crystal structure of the CS-35 F_{ab} fragment, either alone or in complex with a ligand, have been unsuccessful. Therefore, to further probe this important carbohydrate−protein interaction, we have carried out the investigations reported here, which involved a combination of state-of-the-art methods in chemical synthesis, mass spectrometry, and NMR spectroscopy in conjunction with titration microcalorimetry.

Using a panel of 17 synthetic oligosaccharide fragments of mycobacterial arabinan (**4**−**20**, Scheme 1), we used the FAC−MS technique to confirm previous ELISA studies demonstrating that hexasaccharide **4** and tetrasaccharide **8** are CS-35 ligands and that tetrasaccharide **11** is not. In addition, of the three possible pentasaccharide fragments of **4**, only one, **6**, containing residues A, B, C, D, and E was shown to be a CS-35 ligand. Another pentasaccharide, **7** (residues A, B, C, D, and F), is not bound, thus pointing to the importance of residue E in recognition by the antibody. FAC−MS-derived K_{assoc} values showed the hexasaccharide **4** and pentasaccharide **6** bind CS-35 with comparable affinity whereas tetrasaccharide **8** is of lower affinity.

Further characterization of this interaction was carried out using the direct ES−MS method pioneered by Klassen and co-workers for carbohydrate−protein binding.[31−34] Using the F_{ab} fragment of CS-35, these ES−MS studies further confirmed that **4**, **6**, and **8** are bound by the protein and the K_{assoc} values measured, though not in exact agreement with those obtained by FAC−MS, show the same affinity trend: **4** ≈ **6** > **8** (Table 1). These ES−MS studies also showed that both **5** and **7** are also CS-35 ligands, although the latter had not been shown to bind to the antibody using FAC−MS. The K_{assocc} values for **5** and **7** are significantly lower than those for **4**, **6**, and **8** (1−3 orders of magnitude), and so these compounds are relatively weak ligands. Regardless, these results suggest that care must be taken when using the FAC−MS technique for screening potential weak-binding ligands. In addition, these results indicate that for an oligosaccharide to be a strong CS-35 ligand, it must possess not only the non-reducing β-Ara*f* residue E, but also the reducing end α-Ara*f* residue, A. Indeed, the latter seems to be of the greatest importance as its removal leads to a 3 orders of magnitude drop in affinity (cf K_{assoc} of hexasaccharide **4** with that of pentasaccharide **5**), whereas the K_{assoc} of the pentasaccharide lacking residue E (**7**) is only two-orders of magnitude lower than that for **4**. Temperature-dependent binding studies with **4** and **6**−**8** allowed ΔH_{assoc} to be calculated and these showed the same trend as the K_{assoc} values: **4** ≈ **6** > **8** > **7** (Table 1). The binding of both **4** and **8** by CS-35 was also evaluated by titration microcalorimetry and the K_{assoc} values obtained by this method were in excellent agreement with those obtained from the ES−MS experiments (Table 1). However, the absolute values for ΔH_{assoc} for **4** and **8** differed substantially from those obtained from ES−MS.

Further insight was obtained from STD NMR studies between CS-35 F_{ab} and these oligosaccharides. The completion of these studies required first the full assignment of the NMR spectra of the oligosaccharide ligands, which, although complicated due to significant spectral overlap, was possible by careful analysis of spectra obtained from homo- and heteronuclear correlation experiments. This information, in conjunction with previous assignments made on related molecules,[24b] should prove useful as additions to NMR databases that are used for polysaccharide structural elucidation.[61]

STD NMR experiments with the strong binding ligands, hexasaccharide **4**, pentasaccharide **6** and tetrasaccharide **8**, confirmed the results from the ES−MS experiments. That is, that the majority of the saturation transfer was to residues A

(59) Hamasur, B.; Haile, M.; Pawlowski, A.; Schröder, U.; Williams, A.; Hatch, G.; Hall, G.; Marsh, P.; Källenius, G.; Svenson, S. B. *Vaccine* **2003**, *21*, 4081−4093.
(60) Tong, M.; Jacobi, C. E.; van de Rijke, F. M.; Kuijper, S.; van de Werken, S.; Lowary, T. L.; Hokke, C. H.; Appelmelk, B. J.; Nagelkerke, N. J. D.; Hans J. Tanke, van Gijlswijk, R. P. M.; Kolk, A. H. J.; Raap, A. K. *J. Immunol. Meth.* **2005**, *301*, 154−163.
(61) (a) van Kuik, J. A.; Vliegenthart, J. F. *Trends Biotechnol.* **1992**, *10*, 182−185. (b) http://www.eurocarbdb.org/.

and E, with the former having the closest association with the protein. As expected, residues B and C, which link A and E also have significant contact with the protein while the other residues (D and F) appear to only interact slightly. As residue D does not have significant interactions with the protein, the reduction in binding of tetrasaccharide **8** compared to pentasaccharide **6** is unexpected. We propose that this loss of affinity is due to entropic changes in the ligand, and that residue D rigidifies pentasaccharide **6**, which then "pre-organizes" it for binding to the protein. A similar effect can be expected in **4**. Support for the rigidification of **4** and **6** compared to **8** comes from a number of experiments. First, NOE studies with **4** demonstrate that for the terminal residues A and E/F, the NOEs are positive, whereas the central residues B, C, and D display negative NOEs at 500 MHz and 278 K, indicating slower overall motion. Second, the ^{13}C T_1 measurements clearly show that residue B becomes less mobile upon the glycosylation with residues C and D; similar trends are seen for C and D upon attachment of E and F, respectively. Finally, the PSEUROT calculations of **4**, **6**−**8**, and **11** (Table 2 and 3) also show that the conformational equilibria of these core residues are biased to one conformer in the larger more highly branched structures.

The use of the weaker-binding ligands in STD NMR experiments also provided important information. Pentasaccharides **5** and **7** show similar STD patterns, with the majority of the saturation transfer occurring to residues B, C, and E (**5**) or A, B, and C (**7**) and relatively little to residues D and F. Thus, these ligands appear to bind in a manner similar to the strong binders, **4**, **6**, and **8**, and it appears that the absence of residues A or E is responsible for the loss in affinity. On the other hand, another weak binder, **11**, containing residues A, B, D, and F shows a dramatically different pattern, with the bulk of the saturation transfer occurring to residue F. This data suggests that in the absence of residue C, ligands bind in an alternate mode (Figure 9). When presented with a ligand containing residues A, B and C (**4**−**8**), recognition by the antibody appears to occur through the preferred "native" binding mode; however for ligands lacking C, but still possessing a β-Ara*f* residue (necessarily residue F), binding in the alternate mode is observed. Although we demonstrated that **8** and **11** compete for the same binding site, proving the existence of the two-state binding model proposed in Figure 9 will require additional studies. It is intriguing to speculate that in the native binding mode the antibody does not interact with residues D and F of the hexasaccharide to any significant degree and that the saturation transfer observed to these residues in **4** (and to residue D in **6**) is due to the binding of a small fraction of these ligands in this alternate mode. The availability of an X-ray crystal structure of the F_{ab} in complex with one of the ligands will be particularly valuable in determining the feasibility of this hypothesis.

Further STD NMR studies with tetrasaccharide **8**, in which the on-resonance frequency was varied from +7 ppm to +1 ppm, provided information on the nature of the binding pockets. These experiments suggest that residue E interacts predominantly with aliphatic amino acids, whereas residues A, B, and C, an α-(1→5)-linked arabinofuranotriose moiety, are bound by aromatic residues in the protein. With regard to this latter observation, it is interesting to note that recent X-ray crystal structures of α-L-arabinofuranosidases,[18a,b,f] which cleave α-(1→5)-linked plant L-arabinans, possess aromatic amino acids in the sugar binding cleft and thus this may be a common feature of proteins that bind to α-(1→5)-linked Ara*f* motifs. An analogous series of experiments with the weaker-binding tetrasaccharide **11**, also suggested that residue F was bound in an aliphatic pocket, which provides some additional support for the two-state model proposed in Figure 9.

These specificity studies are of interest in light of a recent report[62] in which a phage display peptide library was panned against CS-35 and two peptide mimotopes for the antibody were identified. One, a heptapeptide, was shown to bind to the antibody with an affinity similar to **4** ($K_{assoc} \approx 1 \times 10^5$ M). The other ligand identified was a dodecapeptide, but a K_{assoc} for this compound was not reported. It was suggested that this peptide mimics the hexasaccharide motif at the non-reducing end of LAM and AG, but no competition studies were carried out to establish that these peptides and the oligosaccharide ligands bind to the same site on the protein. The report of the peptide mimotopes for CS-35 prompted us to consider whether other naturally occurring glycans were ligands for the mAb and thus the protein was screened against a 300-member glycan array at the Consortium for Functional Glycomics[63] (data not shown). This screen revealed that none of the glycans present in this library (none of which contain D-Ara*f* residues) had any significant affinity for CS-35; therefore, peptide mimotopes notwithstanding, the antibody appears to be specific for D-Ara*f*-containing glycoconjugates.

In summary, we report here a further refinement of the ligand specificity of the CS-35 antibody, which is widely used in the characterization of polysaccharides containing D-arabinofuranose residues. Through a multi-pronged approach involving chemical synthesis, mass spectrometry, titration microcalorimetry, and NMR spectroscopy, we have established that the binding pocket appears to bind a linear tetrasaccharide motif (tetrasaccharide **8**) and that the terminal two residues, A and E, are essential for strong binding. From the STD NMR studies, we further propose that residue E is bound in an aliphatic pocket and that the bulk of the interactions with residues A, B, and C are with aromatic amino acids. In addition, these studies allow us to make some more provocative hypotheses, which require further study. First, we propose that the enhancement in binding affinity observed in more highly branched structures (**4** and **6**) may be the result of ligand preorganization as the "additional" Ara*f* residues in these larger glycans appear to form relatively few contacts with the protein. Inherent in this proposal is that the strongest binding ligands possess, in addition to residues A and E, a rigid core consisting of residues B, C, and D. Second, our results have allowed us to postulate that ligand binding to the protein may occur through one of two modes as illustrated in Figure 9. Currently underway are investigations directed toward further probing these postulates and chief among these is work directed toward obtaining a crystal structure of **4** in complex with the CS-35 F_{ab} fragment. To date, our efforts in this area have been hampered by a lack of crystals suitable for X-ray crystallography.

Acknowledgment. This work was supported by the Alberta Ingenuity Centre for Carbohydrate Science, The University of

(62) Sharma, A.; Saha, A.; Bhattacharjee, S.; Majumdar, S.; Das, S. K. *Clin. Vaccine Immunol.* **2006**, *13*, 1143−1154.
(63) www.functionalglycomics.org.

Alberta and The Natural Sciences and Engineering Research Council of Canada. J.S.K. thanks the Canadian Foundation for Innovation for their support in the purchase of a 9.4 T magnet for the FTMS instrument. C.R. thanks Drs. Dushan Uhrin, Sven Augner, and Albin Otter for assistance with the CSSF experiments, in the use of DAISY, and fruitful discussions. T.P. acknowledges financial support from the University of Lübeck and from the Deutsche Forschungsgemeinschaft (PE 494/5-1) and HBFG 101/192-1. We also thank NIH−TB contract NO1-AI-75320 and Dr. John S. Spencer for providing the cell line used to produce mAb CS-35 and Professor David F. Smith for screening mAb CS-35 against the glycan array of the Consortium for Functional Glycomics.

Supporting Information Available: Experimental details and data for the preparation of **5**, examples of spectra used to assign resonances in NMR spectra, STD spectra showing the glucose does not bind to CS-35, STD spectra from competition experiment with **8** and **11**, initial slopes data used to probe amino acids present in combining site, tables of NMR resonance assignments, $^{3}J_{H,H}$, and ^{13}C T_1 times. This material is available free of charge via the Internet at http://pubs.acs.org.

JA0723380